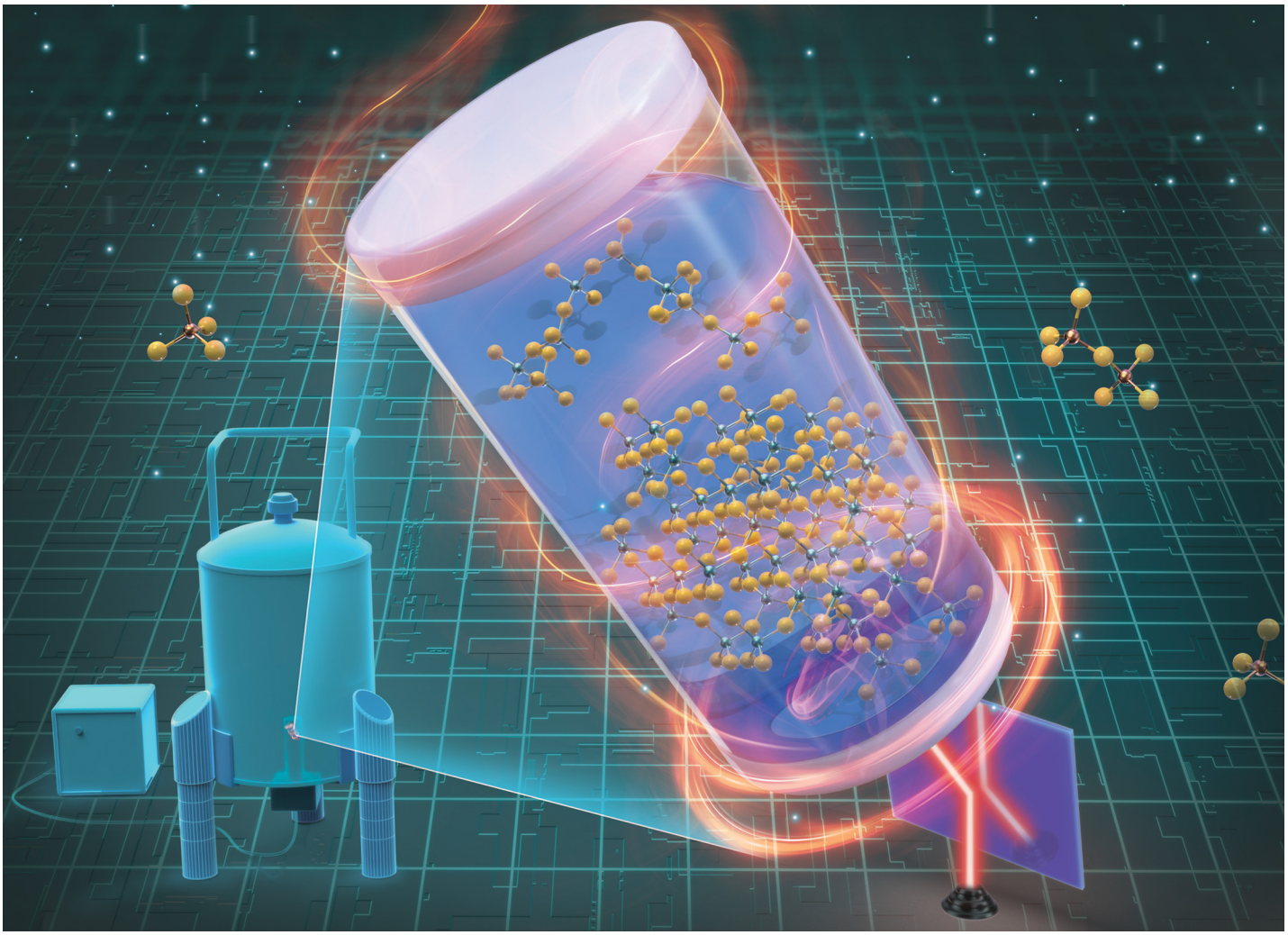

Showcasing research from the Group of Dr Hongtao Liu and Dr Xiaobin Fu at Shanghai Institute of Applied Physics, Chinese Academy of Sciences, China.

Probing the local structure of FLiBe melts and solidified salts by *in situ* high-temperature NMR

The Hongtao group is working on the structure and dynamics of molten salts and other functional materials, and the development of new NMR methods. This work investigates the ionic structure of LiF-BeF_2 melts using *in situ* High-temperature NMR spectrometry by a laser-heating system. With the increase of BeF_2 component, the polymeric Be–F chains and networks were observed, which will be closely related to the thermo-physical properties and their applications in MSR.

As featured in:

See Yuan Qian, Hongtao Liu *et al.*, *Phys. Chem. Chem. Phys.*, 2023, **25**, 19446.

ROYAL SOCIETY OF CHEMISTRY

rsc.li/pccp

Registered charity number: 207890

PCCP Owner Societies

PCCP

PAPER

View Article Online
View Journal | View Issue

Cite this: *Phys. Chem. Chem. Phys.*, 2023, **25**, 19446

Probing the local structure of FLiBe melts and solidified salts by *in situ* high-temperature NMR†

Xiaobin Fu, ‡[a] Yiyang Liu,‡[a] Hailong Huang,[a] Huiyan Wu,[ab] Jianchao Sun,[ab] Ling Han,[ab] Min Ge,[a] Yuan Qian*[a] and Hongtao Liu *[a]

Received 10th March 2023,
Accepted 1st June 2023

DOI: 10.1039/d3cp01096a

rsc.li/pccp

The 2LiF-BeF_2 (FLiBe) salt melt is considered the primary choice for a coolant and fuel carrier for the generation IV molten salt reactor (MSR). However, the basics of ionic coordination and short-range ordered structures have been rarely reported due to the toxicity and volatility of beryllium fluorides, as well as the lack of suitable high-temperature *in situ* probe methods. In this work, the local structure of FLiBe melts was investigated in detail using the newly designed HT-NMR method. It was found that the local structure was comprised of a series of tetrahedral coordinated ionic clusters (*e.g.*, BeF_4^{2-}, $Be_2F_7^{3-}$, $Be_3F_{10}^{4-}$, and polymeric intermediate-range units). Li^+ ions were coordinated by BeF_4^{2-} ions and the polymeric Be–F network through the analysis of the NMR chemical shifts. Using solid-state NMR, the structure of solid FLiBe solidified mixed salts was confirmed to form a 3D network structure, significantly similar to those of silicates. The above results provide new insights into the local structure of FLiBe salts, which verifies the strong covalent interactions of Be–F coordination and the specific structural transformation to the polymeric ions above 25% BeF_2 concentration.

Introduction

There has been renewed interest in the research on high-temperature molten salts over the past decades due to the significant advantage of molten salts in areas related to generation IV nuclear energy *e.g.*, molten salt reactors (MSR),[1–5] concentrating solar power plants (CSP),[6,7] and other clean energy storage industries.[8,9] It is known that many multiply charged metal ions can form coordinated local structures in molten salts, which have important effects on the physical and chemical properties of the melt.[10,11] The local structure was also important for alkali halide liquid salt, and different ionic structures can significantly adjust the ionic diffusion and dynamics, which is strongly coupled to the viscosity, density, and other salt thermophysical properties.[12,13] In the 1960s, FLiBe (2LiF-BeF_2) was employed as the coolant and nuclear fuel carrier for the molten salt reactor experiment (MSRE) project at Oak Ridge National Laboratory (ORNL).[4] Since then, the LiF/BeF_2 binary salt has aroused continuous attention, and the local structure of the FLiBe salt has been widely investigated through theoretical calculation.[14–17] However, relevant experimental studies especially *in situ* studies on the molecular structure of FLiBe have been rarely reported due to the toxicity,[17–19] volatilization of beryllium fluorides,[20] and the lack of suitable high-temperature high-resolution analytical methods.

High-temperature optical absorption spectroscopy, X-ray absorption fine structure (XAFS) spectroscopy, Raman spectroscopy, and Nuclear Magnetic Resonance (NMR) spectroscopy have been widely used in the investigation of the structure of molten salts, which are always combined with theoretical calculations such as molecular dynamics (MD) or *ab initio* molecular dynamics (AIMD).[21] Recently, these high-temperature methods have been reported in research on the structural studies about the alkaline-earth elements, especially magnesium. In 2020, Fei Wu *et al.*[22] used an X-ray scattering perspective and MD simulations to explain the non-Debye–Waller temperature behavior in the intermediate range order for molten $MgCl_2$ and its mixtures with KCl. The result reveals that molten $MgCl_2$ conforms to a network structure rather than an isolated tetrahedral structure. In 2021, Santanu Roy *et al.*[23] employed X-ray scattering and Raman spectroscopy to study the local structure of molten $MgCl_2$. Combined with the AIMD simulations, the five-coordinate $MgCl_5^{3-}$ complex ions were proven to exist in the molten pure $MgCl_2$ and $ZnCl_2$-$MgCl_2$. In addition, the structure of Ni (II) ions in molten $ZnCl_2$-$MgCl_2$ was also investigated by a multimodal approach combining high-temperature ultraviolet-visible absorption spectra,[10] extended XAFS, AIMD simulations, and rate theory of ion exchange. The research reveals that the coordination states of Ni (II) rely on the temperature and content of molten salts. Despite all the above studies on molten salts, the experimental studies on the local structure of beryllium fluoride melts have rarely been reported. It is known that the X-ray method is quite

[a] *Department of Molten Salt Chemistry and Engineering, Shanghai Institute of Applied Physics, Chinese Academy of Sciences, China. E-mail: qianyuan@sinap.ac.cn, liuhongtao@sinap.ac.cn*
[b] *University of Chinese Academy of Sciences, Beijing, 100049, China*

† Electronic supplementary information (ESI) available. See DOI: https://doi.org/10.1039/d3cp01096a

‡ These authors contributed equally.

difficult to apply on the ionic structure studies of beryllium salt melts because of the high X-ray transmittance of Be atoms.[24] Only some theoretical calculation studies on the ionic structure of beryllium melts were reported.[14–17] It has been found that the BeF_2-based beryllium fluoride mixed salts adopt an analogue to SiO_2 and silicates, which shows a 3D network structure with corner-sharing tetrahedrally coordinated Be^{2+} cations.[25] A series of the tetrahedral coordinated ionic clusters (*e.g.*, BeF_4^{2-}, $Be_2F_7^{3-}$, and $Be_3F_{10}^{4-}$) and the polymeric intermediate-range units may exist in FLiBe melts.[15] Furthermore, the distribution of the different species and the thermo-physical properties as a function of composition were discussed through MD simulation.[14–17] Accordingly, systematic experimental local structure studies on LiF/BeF_2 binary salts have been particularly desirable in supporting the rapid development of MSR over the past few years.

Nuclear magnetic resonance (NMR) spectroscopy is a high-resolution and powerful method to examine the microstructure and dynamics of complicated multiple salt systems.[26] With the development of the high-temperature NMR (HT-NMR) method, the research on the ionic structure of molten salts has deepened. In this work, the local structure of FLiBe melts was investigated in detail using a newly designed HT-NMR method. A laser beam coupled with an optical fiber was used to construct the salt heating system for HT-NMR, which was systematically presented in our previous work.[27] The structure and the evolution of different coordinated cluster anions were discussed through the analysis of ^{19}F, ^{7}Li, and ^{9}Be NMR chemical shifts. The strong covalent interactions of Be^{2+} ions were also discussed based on the above results. Furthermore, the structure of solid FLiBe solidified mixed salts at ambient temperature was also investigated by 1D and 2D solid-state NMR (ss-NMR). The network structure of the FLiBe glass state was certified, which should have close relations with the formation and the amount of the polymeric Be–F network during the solidification of FLiBe melts. Our work deepens the understanding of the local structure of FLiBe salts and demonstrates the significant potential of the NMR method on the structural studies of fluoride salts, which is closely related to their applications in the field of the development of new energy production technology.

Experimental section

Sample preparation

The LiF and BeF_2 were purchased from Aladdin. LiF-BeF_2 salts were synthesized as follows: 10 g of salts were weighed in proportion and mixed thoroughly in a nickel crucible sealed with a screw cap; then it was heated to 850 °C by 5 °C min^{-1} and kept for 3 hours in an electrothermal furnace. After that, it was cooled down to room temperature at 5 °C min^{-1} in the furnace. All the operations were carried out in an argon-atmosphere glovebox.

X-ray diffraction

X-ray diffraction measurements were performed on a Bruker D8 ADVANCE using Cu-Kα (1.5406 Å) radiation (40 kV, 20 mA). All samples were mounted on the same sample holder and scanned from $2\theta = 10^\circ$ to 70° at a speed of 10° min^{-1}. To avoid the deliquescence of the salt samples, a Kapton membrane was covered on the sample holder and the background signals are shown in Fig. S3 (ESI†). The experiments were performed at room temperature.

DFT calculation

The quantum chemical calculations of $Be_{(1+n)}F_{(4+3n)}^{(2+n)-}$ (n = 0–3) were carried out using the Gaussian 09 program. The geometries of the anions were fully optimized at the B3LYP/AVTZ level, in which the B3LYP hybrid density functional with the aug-cc-pVTZ (AVTZ) basis set was employed. Frequency analyses were performed at the same level of theory to confirm that the optimized geometries were true minimum points. The ^{19}F, ^{9}Be NMR chemical shifts of F and Be atoms in each anionic species were also calculated at the B3LYP/AVTZ level using the optimized structures.

NMR experiments

All of the ^{19}F, ^{7}Li, and ^{9}Be NMR experiments were performed on a Bruker AVANCE NEO 400 WB spectrometer operated at 376.61 MHz, 155.55 MHz, and 56.24 MHz for ^{19}F, ^{7}Li, and ^{9}Be, respectively. For all the high-temp NMR experiments, a 7.0 mm double-resonance laser-heating HT probe was used. Homemade sample containers were used during the experiments, which were reported in our previous work.[27] The experiment temperature was set to 50 °C above the melting point of each LiF/BeF_2 binary molten salt with different BeF_2 concentrations. The melting points of the samples were obtained from the calculated LiF-BeF_2 phase diagram in Fig. S5 in the ESI.†[25] The experiment temperatures were set to 810 °C (15%), 795 °C (17%), 750 °C (22%), 680 °C (25%), 654 °C (27%), 554 °C (32%), 506 °C (35%), and 499 °C (37%) for LiF/BeF_2 binary salt samples with different BeF_2 concentrations respectively. The experiment temperatures were calculated by using the KBr external standard method. The recycle delay was set to 2 s for all of the ^{19}F, ^{7}Li and ^{9}Be HT-NMR experiments. For the solid-state NMR experiments at room temperature, a 3.2 mm double-resonance magic angle spinning (MAS) probe was used. For single pulse excitation (SP) NMR experiments, the recycle delay was set to 60 s, 5 s, and 30s for ^{19}F, ^{7}Li, and ^{9}Be, respectively. The spinning rate was set to 20 kHz. For ^{19}F-^{7}Li and ^{19}F-^{9}Be HETCOR NMR experiments, the cross polarization time was set to 200 us. The MAS rate was set to 10 kHz. To suppress the spin diffusion, FSLG decoupling was applied during t_1 (the ^{19}F dimension) and the ^{19}F RF field was set to 100 kHz. The ^{19}F, ^{7}Li and ^{9}Be chemical shifts were calibrated using $C_2H_4O_2F_3N$ ($\delta = -74.5$ ppm), the LiCl aqueous solution (1 mol L^{-1}, δ = 0 ppm) and BeF_2 (solid, δ = 0 ppm), respectively.

Results and discussion

To investigate the ionic structure of the FLiBe melts, ^{19}F HT-NMR (Fig. 1a) was firstly performed on LiF/BeF_2 binary salts with different BeF_2 concentrations. The experiment temperature was set to 50 °C above the melting point of each LiF/BeF_2 binary

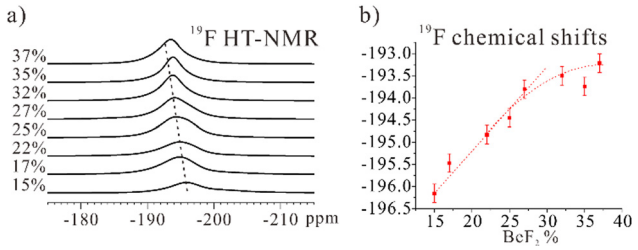

Fig. 1 ^{19}F HT-NMR spectra and chemical shift evolution of LiF-BeF_2 molten salts with different BeF_2 concentrations.

molten salt. Only one signal was observed in each ^{19}F spectrum because of the rapid and dynamic exchange between the different species involving the observed nucleus. The peak position was the average between the chemical shifts of the different units present in the melt weighted by their relative proportions. It was observed that the ^{19}F signal shifted to the low field with the increase of the BeF_2 concentration. To exhibit the changes of the signals clearly, the chemical shift evolution of LiF-BeF_2 molten salts with different BeF_2 concentrations is illustrated in Fig. 1b. To obtain the averaged chemical shifts accurately, signal simulation was carried out and the detailed expatiation is given in the ESI† (Fig. S7 and Tables S1, S2). It is clearly seen that ^{19}F chemical shifts follow an almost linear change when the BeF_2 concentration is below 25%. As reported and described above, the linear change always implies a dynamic exchange of two species due to the average between the two specific chemical shifts. However, when the BeF_2 concentration was above 25%, a non-linear monotonous evolution of the ^{19}F chemical shifts was observed. The deviation thus demonstrated the existence of, at least, a third type of fluorine anion complexes in FLiBe melts.

^{9}Be HT-NMR was also performed on the above salt samples to investigate the coordinated structure of Be^{2+} ions and the chemical shift evolution plot is illustrated in Fig. 2a. Unlike the monotonous evolution of ^{19}F NMR, the plot of ^{9}Be NMR showed quite a different trend. First, with the increase of BeF_2 concentration, the ^{9}Be NMR signal stayed almost unchanged when the BeF_2 concentration was below 25%. This indicates that the chemical structure of Be^{2+} ions also remained unchanged. When the BeF_2 concentration reached 25%, the ^{9}Be NMR signal started to go into high field, suggesting the formation of the new structure species of Be–F complexes. Such a change is also consistent with the ^{19}F NMR results.

As revealed by the ^{19}F and ^{9}Be NMR results, when the BeF_2 concentration is lower than or higher than 25%, the ionic coordinated structure of Be–F ions should be significantly different. The theoretical studies have suggested that BeF_4^{2-} ions will form first and gradually become the main species with the addition of BeF_2 into the LiF salt.[15] At a low BeF_2 concentration, the melt is essentially well-dissociated, and it comprises Li^+, BeF_4^{2-}, and F^- species. With the increase of BeF_2 concentration, BeF_4^{2-} ions continuously increase, and free F^- anions decrease. As a result, the fast exchange between BeF_4^{2-} anions and F^- anions makes the ^{19}F NMR chemical shifts follow a linear variation. Meanwhile, all the Be^{2+} ions form BeF_4^{2-} complexed ions and thus ^{9}Be signal keep almost unchanged. When the BeF_2 concentration reaches 25%, the evolution of ^{19}F and ^{9}Be NMR chemical shifts tend to be particularly different from that lower than 25%, suggesting the formation of the new coordinated ionic structure.

According to the theoretical calculation results by Smith *et al.*,[15] polymeric species (*e.g.*, $Be_2F_7^{3-}$, $Be_3F_{10}^{4-}$, and $Be_4F_{13}^{5-}$) were formed progressively when the BeF_2 concentration increased, until a fully connected network was constructed for pure BeF_2. When BeF_2 concentration was higher than 25%, the polymeric Be–F network tended to be the main species in the FLiBe melt. The formation of the polymeric network should account for the changes in ^{19}F and ^{9}Be evolution. The ionic structure of the BeF_4^{2-} ions and the Be–F polymeric ions are presented in Fig. 2b. The polymeric Be–F network is made of tetrahedral corner-sharing Be^{2+} cations linked by F^- anions. The formation of the network will lead to the increase of corner-sharing Be^{2+} ions and the linked F^-, thus resulting in the different ^{19}F and ^{9}Be NMR chemical shifts.

DFT calculations were carried out to further investigate the relations between ionic structure and the chemical shift variation trend. The calculated average chemical shifts of the NMR signals are listed in Table 1. The detailed calculation results and the data processing method are provided in the ESI† in Fig. S9 and S10. It could be observed that ^{19}F chemical shifts would go into low field when the polymeric ions ($Be_3F_{10}^{4-}$, $Be_4F_{13}^{5-}$) formed while for ^{9}Be HT-NMR signals, it would go into high field with the formation of the polymeric ions. The variation tendency is consistent with the experimental ^{19}F and ^{9}Be HT-NMR results, although the values of the calculated chemical shifts are a little different. Based on the above results, we conclude that at low BeF_2 concentration, the melt comprises the isolated species (F^-, BeF_4^{2-} and $Be_2F_7^{3-}$). With the increase of the concentration, especially after 25%, polymeric Be–F

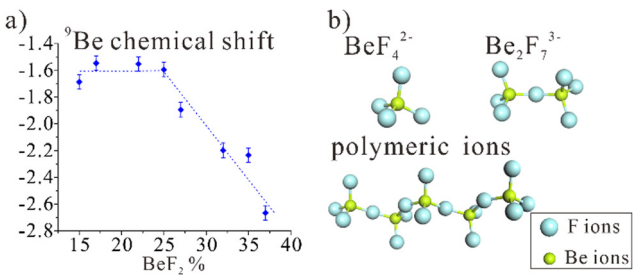

Fig. 2 (a) ^{9}Be HT-NMR chemical shift evolution of LiF-BeF_2 molten salts with different BeF_2 concentrations. (b) Ionic structure of the BeF_4^{2-} ion and the Be–F polymeric ions.

Table 1 DFT calculated average chemical shifts of ^{19}F and ^{9}Be HT-NMR signals of different Be–F coordinated species

	^{19}F c.s./ppm	^{9}Be c.s./ppm
BeF_4^{2-}	−197.44	−1.92
$Be_2F_7^{3-}$	−192.09	−2.28
$Be_3F_{10}^{4-}$	−189.75	−2.37
$Be_4F_{13}^{5-}$	−187.69	−2.38

network ($Be_3F_{10}^{4-}$, $Be_4F_{13}^{5-}$ and even polymer chains) is formed and gradually becomes the main species in the FLiBe melt.

Formation of the polymeric Be–F network should be probably derived from the strong covalent interactions between Be and F atoms. Similar to silica SiO_2 and some silicates,[28,29] the strong interactions can facilitate the formation of tetrahedral network. The similarity between FLiBe and silicates thus illustrates that Be–F bonds should have some covalent properties. As reported in the literature,[13–15] the Be–F distances in FLiBe melts with high BeF_2 concentration is about 1.57 Å, which is calculated *via* MD and AIMD simulation. The relatively short ionic distance thus indicates that the Be–F bonds exhibit the particular covalency. Moreover, compared to Mg, the Be–F interactions are much higher than Mg–F interactions although they are the same alkali earth group atoms. According to the literature,[30] the calculated bond dissociation energy of BeF^- ions is 88.7 kcal/mol, which is also much higher than that of MgF^- ions (61.9 kcal/mol). This could also indicate the strong covalent interactions of Be–F bonds. The strong covalent interactions of Be^{2+} ions thus can facilitate the coordination between Be^{2+} ions and F^- ions, leading to the formation of the network structure in FLiBe melts with high BeF_2 concentration.

Previous work has suggested that Li^+ ions do not form any complex with Be^{2+} or F^- ions.[26] To examine the coordinated structure of Li^+ ions, ^{7}Li HT-NMR was also performed on these FLiBe salt samples and the spectra are presented in Fig. 3a. The evolution of ^{7}Li chemical shifts is also primarily similar to ^{19}F and ^{9}Be results, indicating the formation of the polymeric Be–F networks. Unexpectedly, two broad signals could be distinguished in the spectra of FLiBe melts with 22% and 25% BeF_2 concentration. In these two samples, the melt consists of both BeF_4^{2-} ions and the polymeric Be–F network. The two ^{7}Li signals should be assigned to the Li^+ ions coordinated with the dissociated BeF_4^{2-} ions and the polymeric Be–F network. The separation of the two ^{7}Li signals may be due to the reduced exchange rate of these two species, which is caused by the formation of the polymeric Be–F network. This indicates that Li^+ ions don't simply follow the dissociative state which doesn't form any complex with F^- ions. The two separable ^{7}Li signals thus verified that Li^+ ions should be also coordinated by the dissociated F^-, BeF_4^{2-} ions, and the polymeric Be–F network, respectively. Furthermore, considering the reduced exchange behavior between the two species, we should also observe two signals in the ^{19}F HT-NMR spectra. However, such individual signals were hardly observed due to the relatively low resolution of ^{19}F signals.

Fluoride crystals have wide applications in the optical industry such as luminescence materials and laser crystals. In general, BeF_2 is believed to adopt a structure analogue to SiO_2, with a 3D network of corner-sharing tetrahedrally coordinated structure.[28] The crystal behavior and the glass state of the beryllium fluorides can significantly influence their applications. As discussed above, the addition of alkali-metal elements, LiF, can adjust the ionic structure of FLiBe melts. Formation of the polymeric Be–F network would reduce the crystallization and thus lead to the glass state during the solidification of FLiBe melts.

To investigate the local structure of solidified FLiBe mixed salts, high-resolution solid-state ^{19}F MAS NMR spectroscopy was performed on LiF/BeF_2 salts with different BeF_2 concentrations and the spectra are presented in Fig. 4. Four signals could be observed in the above spectra, which are named F-1 (−205.6 ppm), F-2 (−202.0 ppm), F-3 (−195.8 ppm), and F-4 (−187.3 ppm) respectively. To exhibit the differences of the signals, the software "Dmfit" was employed for signal decomposition and the calculated intensities of the signals are presented in Fig. S2 (ESI†). With the increase of BeF_2 concentration, the intensity of F-1 and F-2 signals tended to decrease gradually and the intensity of the F-3 signal increased. When BeF_2 concentration reached 60%, F-1 and F-2 signals disappeared, and a new F-4 signal appeared in the spectrum. Signal assignment should be conducted to further analyze the local structure of FLiBe mixed salts.

To assign the ^{19}F signals, 2D ^{19}F-^{7}Li and ^{19}F-^{9}Be Heteronuclear Correlation (HETCOR) NMR spectroscopy was performed on the LiF/BeF_2 salts (40% BeF_2) and the spectra are presented in Fig. 5. It could be observed that F-1 (^{19}F) signal has cross peaks with ^{7}Li signal only. No cross peaks could be observed between F-1 and ^{9}Be signals, suggesting the above F^- ions are only bonded to Li^+ ions. Thus, we assign F-1 signal

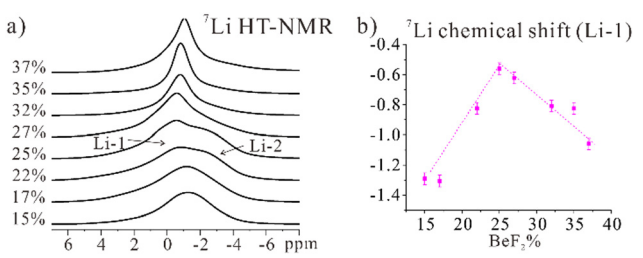

Fig. 3 ^{7}Li HT-NMR spectra and chemical shift evolution of LiF-BeF_2 molten salts with different BeF_2 concentrations.

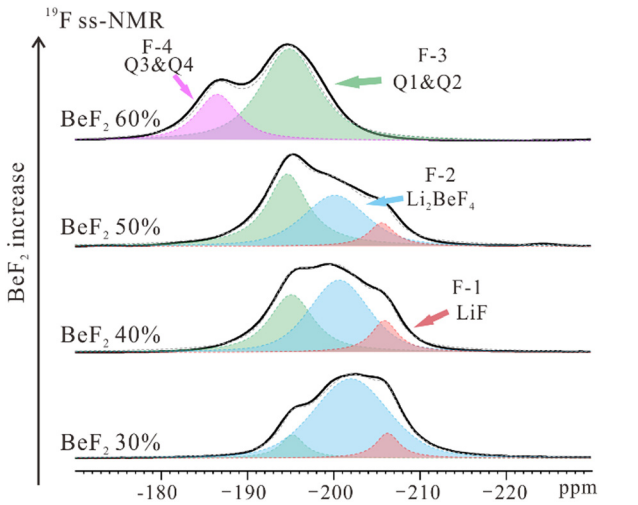

Fig. 4 Solid-state ^{19}F MAS NMR spectra of FLiBe mixed salts with different BeF_2 concentrations. The software "Dmfit" was used for signal decomposition.

to the F^- ions of LiF crystals. For F-2 and F-3 signals, they have cross peaks with both ^{7}Li signal and ^{9}Be signal, indicating that these F^- ions are bonded to Li^+ ions and Be^{2+} ions. It is known that Li_2BeF_4 crystals can be formed when the molar ratio of LiF:BeF_2 is about 2 : 1. To verify if Li_2BeF_4 crystals exist in the mixed salts, XRD was performed on the samples and the XRD patterns are presented in Fig. S3 (ESI†). As shown, the characteristic diffraction peaks of Li_2BeF_4 crystals could be clearly observed, illustrating the existence of Li_2BeF_4 crystal lattices. Thus F-2 signal is assigned to the F^- ions of Li_2BeF_4 crystals.

It was observed that the intensity of F-1 and F-2 signals continuously decreased with increasing the concentration of BeF_2. After the concentration of BeF_2 reached 60%, F-1 and F-2 signals almost disappeared, demonstrating the absence of LiF and Li_2BeF_4 crystals in the salt samples with high BeF_2 concentration. Moreover, the intensity of F-3 signal increased gradually and a new signal F-4 appeared at high BeF_2 concentration. As expected, FLiBe should be also in a glassy state similar to silicate glasses with a 3D network structure (such as Na_2SiO_3). The above results reveal that F-3 and F-4 signals should be assigned to the F^- ions of FLiBe glasses.

In comparison with silicate glasses, Be–F glasses could be also distinguished by these different structure models, which were named Q1, Q2, Q3, and Q4 respectively. The structure models are shown in Fig. 6b. F-4 signal existed only in the ^{19}F ss-NMR spectrum of FLiBe salts with a significantly high BeF_2 concentration and we assign F-4 signal to the F^- ions of Q3 or Q4 model with Be–F 3D networks. For F-3 signal, the signal intensity increased with the increase of BeF_2 concentration. Thus F-3 signal was assigned to the F^- ions of Q1 and Q2 models with Be–F dimers or chains. Changes of the ^{9}Be NMR spectra of LiF-BeF_2 solidified mixed salts with different BeF_2 concentrations also follow the above signal assignment. ^{9}Be ss-NMR spectra and signal simulation of LiF-BeF_2 mixed salts are presented in Fig. 6a. Two signals were observed in the spectra, named Be-1 and Be-2. Be-1 should be the Be^{2+} ions of Li_2BeF_4 crystals and Q1 model with Be–F dimers. Be-2 should be the Be^{2+} ions of Q2, Q3, or Q4 models. The abundant corner-sharing tetrahedrally coordinated Be^{2+} cations of Q2 and Q3 should account for the distinguished chemical shifts of Be-1 and Be-2.

The structure transition of FLiBe solidified mixed salts can be investigated through the above signal assignment of ^{19}F and

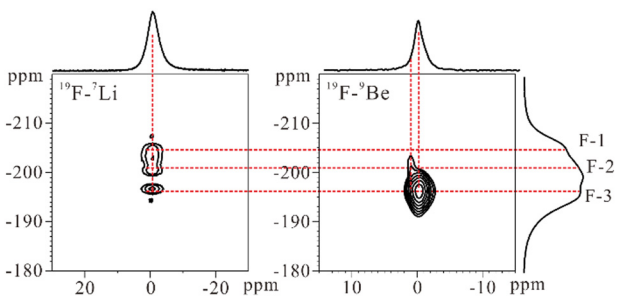

Fig. 5 ^{19}F-^{7}Li and ^{19}F-^{9}Be HETCOR NMR spectra of LiF-BeF_2 salts (40% BeF_2).

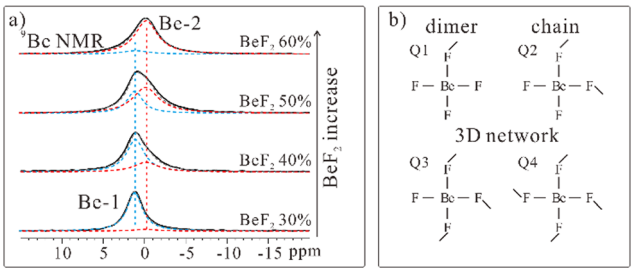

Fig. 6 (a) ^{9}Be NMR spectra and signal simulation of LiF-BeF_2 mixed salts with different BeF_2 concentrations. (b) Illustration of the structure models of Be–F glasses.

^{9}Be ss-NMR. At a low BeF_2 concentration, the LiF-BeF_2 mixed salts consisted of LiF crystals and Li_2BeF_4 crystals. Moreover, there was also a small amount of the oligomer (*e.g.*, Q1 Be–F tetrahedral ions). With the increase of BeF_2 concentration, LiF crystals and Li_2BeF_4 crystals became gradually disordered. Instead, numerous corner-shared Be–F tetrahedra formed and the number of Q1/Q2 structures increased, thus becoming the main species. This should be caused by the strong Be–F covalent interactions, which is quite similar to some silicates. When the BeF_2 concentration was extremely high (>60%), the Be–F network (Q3 and Q4) was also formed, and most the LiF crystals and Li_2BeF_4 crystals disappeared. Obvious signal broadening could be observed of the XRD patterns, indicating a decreased degree of crystallinity. This also illustrates that the main part of the samples transforms into the glass state. Upon further increasing the BeF_2 concentration, the mixed salt would transform completely into the glass state (similar to BeF_2). In addition, the formation of the FLiBe glass state should also have close relations with a large amount of the polymeric Be–F structures. The strong Be–F covalent interactions of the Be–F network of FLiBe melts would reduce the crystallization and thus lead to the formation of FLiBe glass. Upon adding LiF into the system, the alkali metal ions will break the long chains or networks, which is beneficial to the crystallization during the solidification of FLiBe melts. This should be the transition process of LiF-BeF_2 mixed salts from crystals into glasses.

Conclusions

In summary, the local structures of LiF-BeF_2 molten salts and the solidified mixed salts are systematically interpreted in detail using the HT-NMR and solid-state MAS NMR methods. In this study, it was suggested that the strong covalent interactions of Be^{2+} ions can facilitate the coordination between Be^{2+} ions and F^- ions. As a result, polymeric Be–F chains and networks can be formed, which will be closely related to the ionic dynamics. ^{19}F, ^{7}Li, and ^{9}Be NMR experiments were used to understand the local structure and the structural transition of the investigated materials. As revealed from the NMR results, the BeF_4^{2-}, $Be_2F_7^{3-}$, and $Be_3F_{10}^{4-}$ coordinated species as well as the polymeric Be–F chains/networks exist in FLiBe melts, the amounts of which can be adjusted *via* the BeF_2 concentration.

Moreover, the structure of solid FLiBe mixed salts at ambient temperatures was also investigated by 1D and 2D solid-state NMR (ss-NMR). The network structure of FLiBe was verified to be similar to those of silicate glasses. According to the results of the observations, the local structure of FLiBe salts was elucidated using experimental methods, and more insights were provided into the transition of the structure from the isolated ionic systems into the polymeric networks and were found to be significantly related to the thermo-physical properties and their applications in new energy production technology. This work also demonstrates that HT-NMR methods are promising in the investigation of the micro-structure and dynamics of fluoride salts. Our work shows that HT-NMR is also applicable to research on other fluorine-containing materials.

Data availability

The authors declare that data relating to the characterization of materials and products, general methods, experimental procedures, mechanistic studies, XRD data, and NMR spectra are available within the article and the ESI† or from the corresponding author upon request.

Author contributions

Y. Q. and H. L. conceived and designed the experiments. X. F. and Y. L. performed the experiments and analyzed the data. H. H., H. W. and J. S. helped synthesize the BeF_2-LiF salts. L. H. helped draw the structure diagram. X. F. wrote the original manuscript. M. G. helped revise it. All authors proofread the paper, made comments, and approved the manuscript.

Conflicts of interest

There are no conflicts to declare.

Acknowledgements

The authors are grateful for financial support from the National Natural Science Foundation of China (22103094), the K. C. Wong Education Foundation (Grant No. GJTD-2018-10), and the Young Potential Program of Shanghai Institute of Applied Physics, Chinese Academy of Sciences. The authors also express their gratitude to Professor Ian Farnan from the University of Cambridge for his advice on manuscript modification.

Notes and references

1 M. Jiang, H. Xu and Z. Dai, *Bull. Chin. Acad. Sci.*, 2012, **27**, 366–374.
2 H. G. MacPherson, *Nucl. Sci. Eng.*, 1985, **90**, 374–380.
3 J. Serp, M. Allibert, O. Beneš, S. Delpech, O. Feynberg, V. Ghetta, D. Heuer, D. Holcomb, V. Ignatiev, J. L. Kloosterman, L. Luzzi, E. Merle-Lucotte, J. Uhlíř, R. Yoshioka and D. Zhimin, *Prog. Nucl. Energy*, 2014, **77**, 308–319.
4 D. F. Williams, *Assessment of Candidate Molten Salt Coolants for the Advanced High Temperature Reactor (AHTR)*, Oak Ridge, TN, 2006.
5 Y. Wang, J. Tian, S.-W. Wang, C. Zhou and N.-X. Wang, *Nucl. Sci. Tech.*, 2021, **32**, 92.
6 S. Kuravi, J. Trahan, D. Y. Goswami, M. M. Rahman and E. K. Stefanakos, *Prog. Energy Combust. Sci.*, 2013, **39**, 285–319.
7 M. Liu, N. H. Steven Tay, S. Bell, M. Belusko, R. Jacob, G. Will, W. Saman and F. Bruno, *Renewable Sustainable Energy Rev.*, 2016, **53**, 1411–1432.
8 O. Garbrecht, M. Bieber and R. Kneer, *Energy*, 2017, **118**, 876–883.
9 A. Giaconia, M. de Falco, G. Caputo, R. Grena, P. Tarquini and L. Marrelli, *AIChE J.*, 2008, **54**, 1932–1944.
10 S. Roy, Y. Liu, M. Topsakal, E. Dias, R. Gakhar, W. C. Phillips, J. F. Wishart, D. Leshchev, P. Halstenberg, S. Dai, S. K. Gill, A. I. Frenkel and V. S. Bryantsev, *J. Am. Chem. Soc.*, 2021, **143**, 15298–15308.
11 S. Roy, F. Wu, H. Wang, A. S. Ivanov, S. Sharma, P. Halstenberg, S. K. Gill, A. M. Milinda Abeykoon, G. Kwon, M. Topsakal, B. Layne, K. Sasaki, Y. Zhang, S. M. Mahurin, S. Dai, C. J. Margulis, E. J. Maginn and V. S. Bryantsev, *Phys. Chem. Chem. Phys.*, 2020, **22**, 22900–22917.
12 J. Wang, J. Wu, Z. Sun, G. Lu and J. Yu, *J. Mol. Liq.*, 2015, **209**, 498–507.
13 J. Wu, J. Wang, H. Ni, G. Lu and J. Yu, *J. Mol. Liq.*, 2018, **253**, 96–112.
14 J. Dai, H. Han, Q. Li and P. Huai, *J. Mol. Liq.*, 2016, **213**, 17–22.
15 A. L. Smith, E. Capelli, R. J. M. Konings and A. E. Gheribi, *J. Mol. Liq.*, 2020, **299**, 112165.
16 M. Salanne, C. Simon, P. Turq, R. J. Heaton and P. A. Madden, *J. Phys. Chem. B*, 2006, **110**, 11461–11467.
17 R. J. Heaton, R. Brookes, P. A. Madden, M. Salanne, C. Simon and P. Turq, *J. Phys. Chem. B*, 2006, **110**, 11454–11460.
18 D. Naglav, M. R. Buchner, G. Bendt, F. Kraus and S. Schulz, *Angew. Chem., Int. Ed.*, 2016, **55**, 10562–10576.
19 M. Müller and M. R. Buchner, *Angew. Chem., Int. Ed.*, 2018, **57**, 9180–9184.
20 K. A. Sense, M. J. Snyder and J. W. Clegg, *J. Phys. Chem.*, 1954, **58**, 223–224.
21 D. G. Lovering, *Molten Salt Technology*, Springer New York, NY, United States, 1982.
22 F. Wu, S. Sharma, S. Roy, P. Halstenberg, L. C. Gallington, S. M. Mahurin, S. Dai, V. S. Bryantsev, A. S. Ivanov and C. J. Margulis, *J. Phys. Chem. B*, 2020, **124**, 2892–2899.
23 S. Roy, M. Brehm, S. Sharma, F. Wu, D. S. Maltsev, P. Halstenberg, L. C. Gallington, S. M. Mahurin, S. Dai, A. S. Ivanov, C. J. Margulis and V. S. Bryantsev, *J. Phys. Chem. B*, 2021, **125**, 5971–5982.
24 A. Snigirev, I. Snigireva, V. G. Kohn and S. M. Kuznetsov, *Nucl. Instrum. Methods Phys. Res., Sect. A*, 1996, **370**, 634–640.
25 J. R. Allwardt, B. C. Schmidt and J. F. Stebbins, *Chem. Geol.*, 2004, **213**, 137–151.

26 J. K. M. Sanders and B. K. Hunter, *Modern NMR spectroscopy: a guide for chemists*, Oxford University Press, New York, NY, United States, 1988.
27 Y. Liu, R. Lan, C. Dong, K. Wang, X. Fu, H. Liu, Y. Qian and J. Wang, *J. Phys. Chem. C*, 2021, **125**, 4704–4709.
28 I. Farnan and J. F. Stebbins, *Science*, 1994, **265**, 1206–1209.
29 H. Krebs, *Angew. Chem., Int. Ed. Engl.*, 1966, **5**, 544–554.
30 R. Liu, L. Qin, Z. Zhang, L. Zhao, F. Sagan, M. Mitoraj and G. Frenking, *Chem. Sci.*, 2023, **2**, 4872–4887.